HOKKAIDO UNIVERSITY

Title	Ca2+ imaging of cricket protocerebrum responses to air current stimulation
Author(s)	Ogawa, Hiroto; Kajita, Yoriko
Citation	Neuroscience letters, 584, 282-286 https://doi.org/10.1016/j.neulet.2014.10.042
Issue Date	2015-01-01
Doc URL	http://hdl.handle.net/2115/58013
Rights	(C) 2015 Elsevier Ireland Ltd. All rights reserved.
Type	article (author version)
Additional Information	There are other files related to this item in HUSCAP. Check the above URL.
File Information	NL_584_282-.pdf

Instructions for use

Hokkaido University Collection of Scholarly and Academic Papers : HUSCAP

Ca^{2+} imaging of cricket protocerebrum responses to air current stimulation

Hiroto Ogawa[a,b,*] and Yoriko Kajita[c]

[a] Department of Biological Sciences, Faculty of Science, Hokkaido University, Sapporo 060-0810, Japan

[b] PREST, Japan Science and Technology Agency (JST), Kawaguchi 332-0012, Japan

[c] Graduate School of Life Science, Hokkaido University, Sapporo 060-0810, Japan

*Correspondence to: Hiroto Ogawa

Department of Biological Sciences, Faculty of Science, Hokkaido University,

Kita 10-jyo, Nishi 8, Kita-ku, Sapporo 060-0810, Japan

Phone/Fax: +81-11-706-3525

E-mail: hogawa@sci.hokudai.ac.jp

Abstract

Crickets (*Gryllus bimaculatus*) use the cercal sensory system at the rear of the abdomen to detect air currents and direct predator avoidance behavior. Sensory information regarding the direction and dynamic properties of air currents is processed within the terminal abdominal ganglion, and conveyed by ascending giant interneurons (GIs) to higher centers including the brain. However, the brain region responsible for decoding cercal sensory information has not yet been identified, nor the response properties within the brain characterized. In this study, we performed in vivo Ca^{2+} imaging to investigate wind-evoked neural activities within the cricket protocerebrum. Ca^{2+} responses to air current stimuli were observed at peripheral regions of the ventrolateral neuropile (VLNP) where projection of GIs' axon terminals has been observed in larvae. The wind-evoked Ca^{2+} response had temporal dynamics and directional sensitivity that varied with different recorded regions displaying transient or sustained Ca^{2+} increases. Individual cells showed Ca^{2+} elevation in response to air currents from a specific angle, while stimuli from a different angle evoked decreased signals. Removing the antennae reduced the air-current-evoked responses in VLNP, suggesting contribution of sensory inputs from antennae in addition to the cercal inputs. The VLNP is presumably an integrative center for mechanosensory processing from antennae and cerci where directional information is primarily decoded by protocerebral

neurons.

Keywords

Calcium imaging; Directional selectivity; Insect; Protocerebrum; Sensory processing; Mechanosensory system

Highlights

- Air currents evoked Ca^{2+} responses in the ventrolateral neuropile of cricket brain.
- Temporal profiles of Ca^{2+} responses varied across recorded locations.
- Wind-sensitive brain neurons displayed variable sensitivity to stimulus direction.
- Air currents from a specific direction evoked decremental Ca^{2+} responses.

1. Introduction

To accurately perceive the environment, sensory signals detected by various sense organs are hierarchically processed by different brain subdivisions. In the insect nervous system, visual input from the compound eye is primarily encoded by neural circuits of the optic lobe [4,35], and chemical signals sensed by antennae are conveyed to the antennal lobe, which is the primary olfactory center of insect brains [6,16]. In contrast, primary sensory circuits for input provided by thoracic and abdominal sensory organs are located within the lower ganglia. For example, in the cricket, auditory input from the tympanal organ is processed by sound-sensitive interneurons within the prothoracic ganglion [7], and the primary neural circuitry of the cercal sensory system that detects surrounding air currents is located within the terminal abdominal ganglion (TAG) [10].

Cerci form a mechanoreceptive organ consisting of a pair of antenna-like appendages covered with various types of mechanoreceptors. Air currents in the immediate vicinity move filiform hair sensilla on the cercus and activate sensory neurons at their base that exhibit directional and dynamic sensitivity based on biomechanical properties of the hairs [30]. In the house cricket *Acheta domesticus*, 500–750 hairs with diverse directional sensitivity are distributed on each cercus [18,26]. The axons of all receptor afferents project in an orderly array into the TAG to form a functional representation or topographic map of

air current direction [3,12,13,27]. This sensory information is transmitted to primary ascending interneurons, including the giant interneurons (GIs), which are also sensitive to the direction and dynamics of air current stimuli [11,19,23,36,37]. In larvae of the cricket *Gryllus bimaculatus*, it has been identified that GIs project to motor centers in the thorax and integrative centers in the brain [8], but the subregion within the brain ganglion that receives synaptic input from GIs has yet to be identified.

Air currents detected by cerci can elicit at least 14 distinct responses, including evasion, flight, offensive reactions, scanning, freezing, and others, depending on the behavioral state of the animal as well as environmental context [2,5]. This implies that ascending cercal sensory information is integrated with sensory input from other modalities within a higher center that includes the protocerebrum. It was recently reported that directional control of wind-elicited walking behavior requires descending signals from the cephalic ganglia [20], and it is suggested that directional information conveyed by GIs are processed within the brain, in which some multimodal local and descending interneurons responsive to cercal stimulation have been identified [28,31]. However, the specific brain region to which GIs transmit cercal sensory information is not known, and neuronal response properties including directional selectivity have not been investigated within the brain. In this study, in vivo Ca^{2+} imaging was performed of the brain during stimulation by air currents from

various directions. We specifically focused on the brain region known as the ventrolateral neuropile (VLNP), which contains the ventrolateral protocerebrum where projections of GIs' axon terminals have been observed in larvae of *G. bimaculatus* and adults of the bushcricket *Tettigonia cantans* [8,29], and examined response properties of wind-evoked responses in this region.

2. Materials and methods

Loading of the Ca^{2+}–sensitive dye and in vivo Ca^{2+} imaging were performed as previously described [21-25]. The naming of brain regions and neuropiles and axonal dimensions (ventro–dorsal and antero–posterior axes) for the brain ganglion followed the nomenclature conventions established by the Insect Brain Name Working Group [9].

2. 1. Dye loading

Experiments were performed using laboratory-bred, adult male crickets (*G. bimaculatus*). Procedure of the dye loading was similar to the method for microinjection of DNA plasmid for electroporation in our previous work [17]. After crickets were anesthetized by cooling on crushed ice, the wings and legs were removed and the body was pinned dorsal side up on a silicone platform. To expose the brain, part of the head cuticle was carefully removed. For bulk loading of the fluorescent Ca^{2+} indicator, a glass micropipette filled with a solution containing 0.05 % Oregon Green 488 BAPTA-1 (OGB-1) acetoxy-methyl ester, 0.01 % dextran-conjugated Texas Red (10,000 MW), and 0.2% PowerLoad concentrate (X100), dispersing reagent (all chemicals from Life Technologies, Carlsbad, CA, USA) was inserted just under the sheath of the brain at the center of the VLNP in the left hemisphere of the protocerebrum using a micromanipulator. The dye solution was

pressure-injected through the micropipette under the stereomicroscope for checking the dye spreading visually. The injection volume was controlled so that the dye spreading was restricted within left half hemisphere of protocerebrum. The Ca^{2+} fluorescence was visualized 12 h later.

2. 2. Air current stimulation

Air current stimuli were delivered as a short puff of N_2 gas from a 13-mm-diameter plastic nozzle. The duration and velocity of the air puff were controlled at 500 ms and 0.840 ± 0.03 m/s measured at the cricket, respectively, by a pneumatic picopump (PV230, World Precision Instruments, Sarasota, FL, USA) connected to the gas cylinder. Eight nozzles were arranged around the cricket on the same horizontal plane with angle of 45° between nozzles at a distance of 35 mm from the center of the cricket's abdomen. The stimulus direction from the anterior side was defined as 0°, with positive and negative angles corresponding to clockwise (right side of the cricket) and counterclockwise (left side) directions, respectively.

2. 3. High-speed confocal Ca^{2+} imaging

Fluorescence images (512 × 512 pixels) were captured at 33 frames/s with an electron-multiplying charge-coupled device camera (iXon DU897, Oxford Instruments, Abingdon, UK) attached to an upright epifluorescence microscope (E600FN, Nikon Instech, Tokyo, Japan) combined with a Nipkow disk confocal unit (CSU-10; Yokogawa Electric, Tokyo, Japan). For excitation of OGB-1, the brain was illuminated at 488 nm with a 20-mW laser diode (HPU50101, TITEL, Tokyo, Japan). Fluorescence was visualized through a 10× (0.3 NA) water immersion objective lens (Nikon Instech) and the dichroic FT500/bandpass emission 525/40 filter combination. Images were acquired using Andor IQ software (Oxford Instruments, Abingdon, UK), and changes in fluorescence intensity over time were analyzed with BV-Ana custom software (BrainVision, Tokyo, Japan). Changes in cytosolic Ca^{2+} concentration ($[Ca^{2+}]_i$) were calculated using the formula $\Delta F/F$ [$\Delta F/F = (F - F_0) / F_0$], where F_0 is the background-corrected pre-stimulus fluorescence intensity.

3. Results

3. 1. Temporal profile of Ca^{2+} responses in the VLNP to air current stimuli

OGB-1 labeling of the protocerebrum showed fluorescence spots resembling cell bodies in the ventrolateral peripheral region of the VLNP (Fig. 1A, right). According to stack of confocal images sectioned at different focal planes, up to 400 cells were labeled in VLNP of brain hemisphere (Supplementary Fig. 1). Although precise number of neurons within VLNP of the cricket brain has been unknown yet, the ~930 cell bodies have been identified in ventro-lateral protocerebrum for half of fly brain [34]. Therefore, about 40% of cells may be labeled with OGB-1 AM. For high-speed imaging, we acquired time series of images at single focal plane in which the fewer cells were observed simultaneously than all labeled cells.

In the focal plane shown in Fig. 1A, air current stimuli to the cerci evoked a local increase in fluorescence. To localize the response within the VLNP, changes in fluorescence in a square region of interest (ROI), which was similar in size to cell bodies (20 × 20 μm; Fig. 1B, inset) were assessed. Prominent increases in Ca^{2+} that were more than 5 % elevation in relative fluorescence changes ($\Delta F/F$) were detected in five different ROIs, which were assigned to responding cells. The time course of the Ca^{2+} increase varied between these cells (Fig. 1B, right). In ROIs #1 and #2, cytosolic Ca^{2+} concentration

($[Ca^{2+}]_i$) increased gradually during stimulation. The amplitudes of relative fluorescence change were 10.00 and 12.46 % for ROIs #1 and #2, respectively. The delay from stimulus onset to the Ca^{2+} peak was 680 ms in both ROIs. After the air current was terminated, $[Ca^{2+}]_i$ peaked and then slowly declined. The time constant of the Ca^{2+} decay was 1000 ms. In contrast, in ROIs #3 and #4, rapid, transient increases in $[Ca^{2+}]_i$ (amplitude: 8.96 and 9.22 % in $\Delta F/F$, delay to peak: 80 and 170 ms) were observed in response to the air current, with the signal declining before the termination of the stimulus (decay time constant: 143 and 250 ms). ROI #5 also showed a rapid increase in $[Ca^{2+}]_i$ (amplitude: 10.9 % in $\Delta F/F$, delay to peak: 380 ms) and the elevated level (8-11 % in $\Delta F/F$) was sustained for the stimulus duration. After the stimulation was terminated, the Ca^{2+} elevation was long-lasting (decay time constant: 2500 ms). These distinct temporal profiles of the Ca^{2+} response suggest a variety of wind-evoked activity patterns in neurons within the VLNP cercal sensory processing circuit.

3. 2. Directional selectivity of VLNP neurons

To examine the directional sensitivity of wind-responsive cells, air currents were applied from eight different directions and wind-evoked Ca^{2+} signals were recorded. Cells located at different regions within the VLNP exhibited different sensitivity to the stimulus direction

(Fig. 2). Interestingly, in addition to increases in Ca^{2+} level, negative changes in $[Ca^{2+}]_i$ were also observed in the responses to stimuli from specific directions (Fig. 2A). For example, air currents from 45° and −135° angles caused decreases in fluorescence relative to the prestimulation level in ROIs #1 and #2 (–7 to –8 % in $\Delta F/F$). In ROIs #4 and #5, a transient decrease in $[Ca^{2+}]_i$ was induced by a stimulus delivered from the left side (−90°) (–6 to –7 % in $\Delta F/F$). These changes likely reflect suppression of spontaneous spike activity by inhibitory inputs.

The sharpness and shape of the directional tuning curves also differed among cells (Fig. 2B). Cells in ROIs #3–#5 selectively responded to stimuli presented from the front (0°). In contrast, Ca^{2+} signals measured in ROIs #1 and #2 displayed more complex directional tuning. The cell in ROI #1 had broad sensitivity along a diagonal axis from 135° to −45°, while the one in ROI #2 responded to stimuli from front-to-ipsilateral angles (−90° to 0°) and was also sensitive to stimuli from an angle contralateral to the recorded side (90°). This complex tuning to stimulus direction may result from higher order processing by neural circuits in the protocerebrum.

3. 3. Spatial distribution of wind-responsive cells

Air current stimuli applied from eight different directions evoked Ca^{2+} signals in 65 ROIs that were assigned to the responding cells in five different animals in total. The locations of responsive cells were mapped in a schematic of the left hemisphere of the protocerebrum (Supplementary Fig. 2). The majority of cells responded to stimuli from the front (0°), while a few cells were responsive to stimuli from behind (135°, 180°, and −135°). Furthermore, stimuli from the side contralateral to the recorded hemisphere (90°) induced Ca^{2+} elevation in more cells than those delivered from the ipsilateral side (−90°). Most wind-responsive cells were distributed at the inferior lateral margins of the VLNP. Some cells sensitive to stimuli from the contralateral side (90°) were clustered at the posterior medial edge. Cells located close to each other displayed similar directional tuning, as shown in ROIs #3–#5; however, there was no specific pattern to the locations of cells for other stimulus directions. Therefore, the cell body location is unlikely to be related to the directional sensitivity of the cell.

The fact that most of cells responded to the stimuli from rostral but not from caudal side suggests the contribution of antennal inputs to the air-current evoked Ca^{2+} signals. The antennae are mechanosensitive and possibly respond to the air currents delivered from frontal nozzle. Using extracellular recording from VLNP, we compared the firing responses between intact and the antennae-removed preparation, because it was technically difficult to

sever both antennae during the imaging experiment without misalignment of captured images. Ablation of both antennae reduced the number of spikes evoked by air current delivered from front (Supplementary Fig. 3). In turn, removing the cerci also largely diminished spike response to the air currents, which still evoked spike firing in VLNP. This result demonstrates that mechanosensory inputs from the antennae also contribute to the air-current-evoked neural response in VLNP as well as the cercal sensory inputs.

4. Discussion

Ca^{2+} imaging of the cricket protocerebrum revealed air current-evoked neural activity in the peripheral region of the VLNP. Most of the responding ROIs were distributed at the inferior margin of the VLNP where air current-sensitive ascending neurons—including GIs—arborize their axon terminals [8,29]. As shown by Supplementary Fig. 1, the bulk loading of AM types of Ca^{2+} indicator dye labeled cell bodies but not neurite- or axon-like fibers. The cell bodies may more easily uptake the AM ester of Ca^{2+} dye than neurites or axons. In this study, therefore, we focused on the fluorescence signals of the labeled cell bodies. The prominent and rapid Ca^{2+} signals evoked by air current stimuli suggest that the VLNP contains air current-sensitive neurons that receive synaptic input from cercal ascending interneurons, including GIs. Although the axonal projection of GIs has been identified in larvae (3rd instar) of *G. bimaculatus* [8], the morphology and detailed projection area of GIs within the protocerebrum have not been clarified in adult crickets. Long-distance staining of whole GI and confocal imaging will provide more knowledge on spatial relationship between GIs morphology in the brain and air-current-evoked activity.

Ca^{2+} responses to air current had different time courses in different ROIs. This diversity suggests that various temporal patterns of neural activity such as transient and sustained responses are simultaneously evoked in this brain region. Cells located at inferior

edge of the VLNP showed transient Ca^{2+} elevation, which was similar to Ca^{2+} responses in GIs measured in TAG [23,25], implying that excitatory inputs from GIs induce transient bursts of action potentials in these neurons. In contrast, cells in the lateral region of the VLNP such as ROIs #1 and #2 in Fig.1 showed slower changes in $[Ca^{2+}]_i$ than those in other regions such as ROIs #3–#5. This could reflect a sustained firing response that persists after the stimulus has ceased. Some extrinsic mushroom body neurons exhibit long-lasting discharges to cercal stimulation and arborized their bouton-like terminals in the lateral protocerebrum, which corresponds in terms of position to the VLNP [28]. In the cockroach that also has cercal sensory system, mushroom body efferent neurons with arborization in the VLNP responded to mechanical stimulation of the cercus [14,15]. These studies in cricket and cockroach brains have suggested that cercal sensory information could be conveyed to the mushroom body for integration with information of other sensory modalities. The slow Ca^{2+} signals monitored in lateral region of VLNP may indicate neural activity induced by output from the mushroom body.

The transient decreases in $[Ca^{2+}]_i$ may indicate that inhibitory signals were induced by air current delivered from specific directions. Such signals have not been observed among the Ca^{2+} responses of GIs and cercal afferents [24,25]. Reduction of spontaneous spike activity may cause these negative Ca^{2+} signals, because the previous imaging study in TAG

has demonstrated that Ca^{2+} influx through the voltage-gated channels mainly contributes to Ca^{2+} elevation in GIs, and that subthreshold EPSP did not produce the detectable Ca^{2+} signal [22]. Probably, Ca^{2+} decrease directly caused by IPSPs would be undetectable. In the cockroach, stimulation of the cercus suppressed spontaneous firing activity in the efferent interneuron of the mushroom body [15]. Also in crickets, it is possible that air current stimulation to cerci may evoke inhibitory responses in the VLNP neurons via mushroom body outputs. The inhibitory processing may contribute to complex tuning to stimulus direction, as shown in ROIs #1 and #2 (Fig. 2). Most cercal ascending interneurons have simple directional tuning curves with a single peak [1,10,19]. Further electrophysilogical experiments using intracellular recording and anatomical studies would reveal the details of the neuronal circuit that achieves complex processing, including direction-specific inhibition, in the VLNP.

There was no clear relationship between the recorded region and directional preference in air current-evoked responses. It has been suggested that stimulus direction is not represented topographically in the protocerebrum, unlike in the TAG [12,13,27]. More cells responded to air currents from the front than from behind; however, cercal sensory afferents and ascending interneurons including GIs have low sensitivity to stimuli directly in front of the animal [1,10,18]. As suggested by the reduction of the spike responses in the

antennae-removed experiments, these cells could be activated by mechanosensory input from antennae stimulated by air currents. Neuronal tracts from the primary projection area of mechanosensory afferents from the antennae—known as the ventral area of flagellar afferents [32,33]—terminated in the lateral protocerebrum, which corresponds to the lateral region of the VLNP [38]. Therefore, it is possible that the VLNP functions as an integrative center of input from mechanosensory sensilla and organs, including antennae and cerci.

In conclusion, the present work indicates that the VLNP in the protocerebrum is presumably an integrative center for mechanosensory processing of air current information received from antennae and cerci. The labeling method that was used did not permit the identification of individual cell morphology. More selective or sparse loading of cells with dye will allow us to definitively identify the protocerebral neurons involved in cercal sensory processing.

Supplementary information

Supplementary information includes Supplemental Methods and three figures.

Acknowledgements

This work was supported by Japan Science and Technology Agency (JST), Precursory Research for Embryonic Science and Technology (PRESTO) to H.O., and JSPS and MEXT KAKENHI grant 2644017604 to H.O.

References

[1] Y. Baba, K. Hirota, T. Yamaguchi, Morphology and response properties of wind-sensitive non-giant interneurons in the terminal abdominal ganglion of crickets, Zool. Sci. 8 (1991) 437-445.

[2] Y. Baba, T. Shimozawa, Diversity of motor responses initiated by a wind stimulus in the freely moving cricket*, Gryllus bimaculatus*, Zool. Sci. 14 (1997) 587-594.

[3] J.P. Bacon, R.K. Murphey, Receptive fields of cricket giant interneurones are related to their dendritic structure, J. Physiol. (Lond) 352 (1984) 601-623.

[4] A. Borst, Drosophila's view on insect vision, Curr. Biol. 19 (2009) R36-47.

[5] J. Casas, O. Dangles, Physical ecology of fluid flow sensing in arthropods, Ann. Rev. Entomol. 55 (2010) 505-520.

[6] B.S. Hansson, M.C. Stensmyr, Evolution of insect olfaction, Neuron 72 (2011) 698-711.

[7] B. Hedwig, Pulses, patterns and paths: neurobiology of acoustic behaviour in crickets, J. Comp. Physiol. A 192 (2006) 677-689.

[8] K. Hirota, Y. Sonoda, Y. Baba, T. Yamaguchi, Distinction in morphology and behavioral role between dorsal and ventral groups of cricket giant interneurons, Zool. Sci. 10 (1993) 705-709.

[9] K. Ito, K. Shinomiya, M. Ito, J.D. Armstrong, G. Boyan, V. Hartenstein, S. Harzsch, M. Heisenberg, U. Homberg, A. Jenett, H. Keshishian, L.L. Restifo, W. Rössler, J.H. Simpson, N.J. Strausfeld, R. Strauss, L.B. Vosshall; Insect Brain Name Working Group, A systematic nomenclature for the insect brain, Neuron 81 (2014) 755-765.

[10] G.A. Jacobs, J.P. Miller, Z. Aldworth, Computational mechanisms of mechanosensory processing in the cricket, J. Exp. Biol. 211 (2008) 1819-1828.

[11] G.A. Jacobs, J.P. Miller, R.K. Murphey, Cellular mechanisms underlying directional sensitivity of an identified sensory interneuron, J. Neurosci. 6 (1986) 2298-2311.

[12] G.A. Jacobs, F. Theunissen, Functional organization of a neural map in the cricket cercal sensory system, J. Neurosci. 16 (1996) 769-784.

[13] G.A. Jacobs, F.E. Theunissen, Extraction of sensory parameters from a neural map by primary sensory interneurons, J. Neurosci. 20 (2000) 2934-2943.

[14] Y. Li, N.J. Strausfeld, Morphology and sensory modality of mushroom body extrinsic neurons in the brain of the cockroach, *Periplaneta americana*, J. Comp. Neurol. 387 (1997) 631-650.

[15] Y. Li, N.J. Strausfeld, Multimodal efferent and recurrent neurons in the medial lobes of cockroach mushroom bodies, J. Comp. Neurol. 409 (1999) 647-663.

[16] J.P. Martin, A. Beyerlein, A.M. Dacks, C.E. Reisenman, J.A. Riffell, H. Lei, J.G. Hildebrand, The neurobiology of insect olfaction: sensory processing in a comparative context, Prog. Neurobiol. 95 (2011) 427-447.

[17] S.C. Matsumoto, H. Shidara, K. Matsuda, T. Nakamura, T. Mito, Y. Matsumoto, K. Oka, H. Ogawa, Targeted gene delivery in the cricket brain, using *in vivo* electroporation. J. Insect Physiol. 59 (2013) 1235-1241.

[18] J.P. Miller, S. Krueger, J. Heys, T. Gedeon, Quantitative characterization of the filiform mechanosensory hair array on the cricket cercus, PLoS ONE 6 (2011) e27873.

[19] J.P. Miller, F.E. Theunissen, G.A. Jacobs, Representation of sensory information in the cricket cercal sensory system. I. Response properties of the primary interneurons, J. Neurophysiol. 66 (1991) 1680-1689.

[20] M. Oe, H. Ogawa, Neural basis of stimulus-angle-dependent motor control of wind-elicited walking behavior in the cricket *Gryllus bimaculatus*, PLoS ONE 8 (2013) e80184.

[21] H. Ogawa, Y. Baba, K. Oka, Dendritic Ca^{2+} transient increase evoked by wind stimulus in the cricket giant interneuron, Neurosci. Lett. 275 (1999) 61-64.

[22] H. Ogawa, Y. Baba, K. Oka, Spike-dependent calcium influx in dendrites of the cricket giant interneuron. J. Neurobiol. 44 (2000) 45-56.

[23] H. Ogawa, Y. Baba, K. Oka, Directional sensitivity of dendritic calcium responses to wind stimuli in cricket giant interneurons, Neurosci. Lett. 358 (2004) 185-188.

[24] H. Ogawa, G.I. Cummins, G.A. Jacobs, J.P. Miller, Visualization of ensemble activity patterns of mechanosensory afferents in the cricket cercal sensory system with calcium imaging, J. Neurobiol. 66 (2006) 293-307.

[25] H. Ogawa, G.I. Cummins, G.A. Jacobs, K. Oka, Dendritic design implements algorithm for synaptic extraction of sensory information, J. Neurosci. 28 (2008) 4592-4603.

[26] J. Palka, R. Levine, M. Schubiger, The cercus-to-giant interneuron system of crickets. I. Some aspects of the sensory cells, J. Comp. Physiol. 119 (1977) 267-283.

[27] S. Paydar, C.A. Doan, G.A. Jacobs, Neural mapping of direction and frequency in the cricket cercal sensory system, J. Neurosci. 19 (1999) 1771-1781.

[28] K. Schildberger, Multimodal interneurons in the cricket brain: properties of identified extrinsic mushroom body cells, J. Comp. Physiol. A 154 (1984) 71-79.

[29] J. Shen, The cercus-to-giant interneuron system in the bushcricket *Tettigonua cantans*: Morphology and response to low-frequency sound, J. Comp. Physiol. A 151 (1983) 449-459.

[30] T. Shimozawa, M. Kanou, Varieties of filiform hairs: range fractionation by sensory afferents and cercal interneurons of a cricket, J. Comp. Physiol. A 155 (1984) 485-493.

[31] E.M. Staudacher, Sensory responses of descending brain neurons in the walking cricket, *Gryllus bimaculatus*, J. Comp. Physiol. A 187 (2001) 1-17.

[32] E.M. Staudacher, M. Gebhardt, V. Dürr, Antennal movements and mechanoreception: Neurobiology of active tactile sensors, Adv. Insect Physiol. 32 (2005) 49-205.

[33] E.M. Staudacher, K. Schildberger, A Newly described neuropile in the deutocerebrum of the cricket: Antennal afferents and descending interneurons, Zoology: Anal. Complex Systems 102 (1999) 212-226.

[34] N.J. Strausfeld, Atlas of an insect brain, Springer-Verlag, Berlin, Heidelberg, New York, Tokyo (1976).

[35] N.J. Strausfeld, Brain organization and the origin of insects: an assessment, Proc. Biol. Sci. 276 (2009) 1929-1937.

[36] F.E. Theunissen, J.P. Miller, Representation of sensory information in the cricket cercal sensory system. II. Information theoretic calculation of system accuracy and optimal tuning curve widths of four primary interneurons, J. Neurophysiol. 66 (1991) 1690-1703.

[37] F. Theunissen, J.C. Roddey, S. Stufflebeam, H. Clague, J.P. Miller, Information theoretic analysis of dynamical encoding by four primary sensory interneurons in the cricket cercal system, J. Neurophysiol. 75 (1996) 1345-1376.

[38] A. Yoritsune, H. Aonuma, The anatomical pathways for antennal sensory information in the central nervous system of the cricket, *Gryllus bimaculatus*, Invertebr. Neurosci. 12 (2012) 103-117.

Figure legends

Fig. 1

Ca^{2+} responses to air current stimuli in the VLNP. (A) Frontal (anterior) view of an exposed brain ganglion in the cricket. The right panel shows a confocal image of the VLNP region labeled with OGB-1 acetoxy-methyl ester. Scale bar = 200 μm. (B) Ca^{2+} elevation in the VLNP evoked by an air current stimulus applied from the anterior side (0°). The left panel shows a pseudo-colored image of the Ca^{2+} signal superimposed onto the raw fluorescence image before stimulation. Traces in the right panel show the time course of changes in ΔF/F in five ROIs, which encompass fluorescent signals measured in somata at the peripheral part of the VLNP (inset). The pseudo-colored image was acquired at the time point indicated by the broken line in the right panel. Horizontal scale bars = 100 μm (left), 20 μm (inset), and 500 ms (right); vertical scale bar = 10% in ΔF/F.

Fig. 2

Directional sensitivity in Ca^{2+} responses of the VLNP. (A) Time course of changes in fluorescence in five different ROIs indicated in the upper left image. Air currents were delivered from eight different directions for 500 ms. The upper right diagram indicates the stimulus direction with respect to the cricket. The direction of stimuli from the side

contralateral to the recorded hemisphere and from the ipsilateral side are indicated as positive degrees (clockwise) and negative degrees (counterclockwise), respectively, from the anterior of the cricket. Horizontal scale bar = 500 ms; vertical scale bar = 4% in $\Delta F/F$. (B) Directional tuning curves of Ca^{2+} responses in different regions. Polar plots show the amplitude of air current-evoked Ca^{2+} signals with respect to stimulus orientation. Each Ca^{2+} response value was scaled to the maximal response of each measurement. Plots in shaded areas indicate negative peak value in Ca^{2+} decrease responses. The number above each plot corresponds to ROIs measured in (A).

Fig. 1

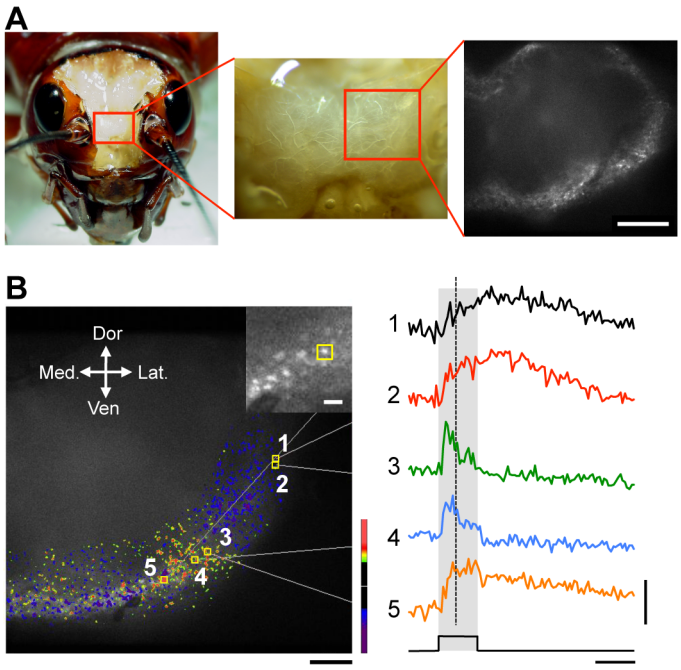

Fig. 2

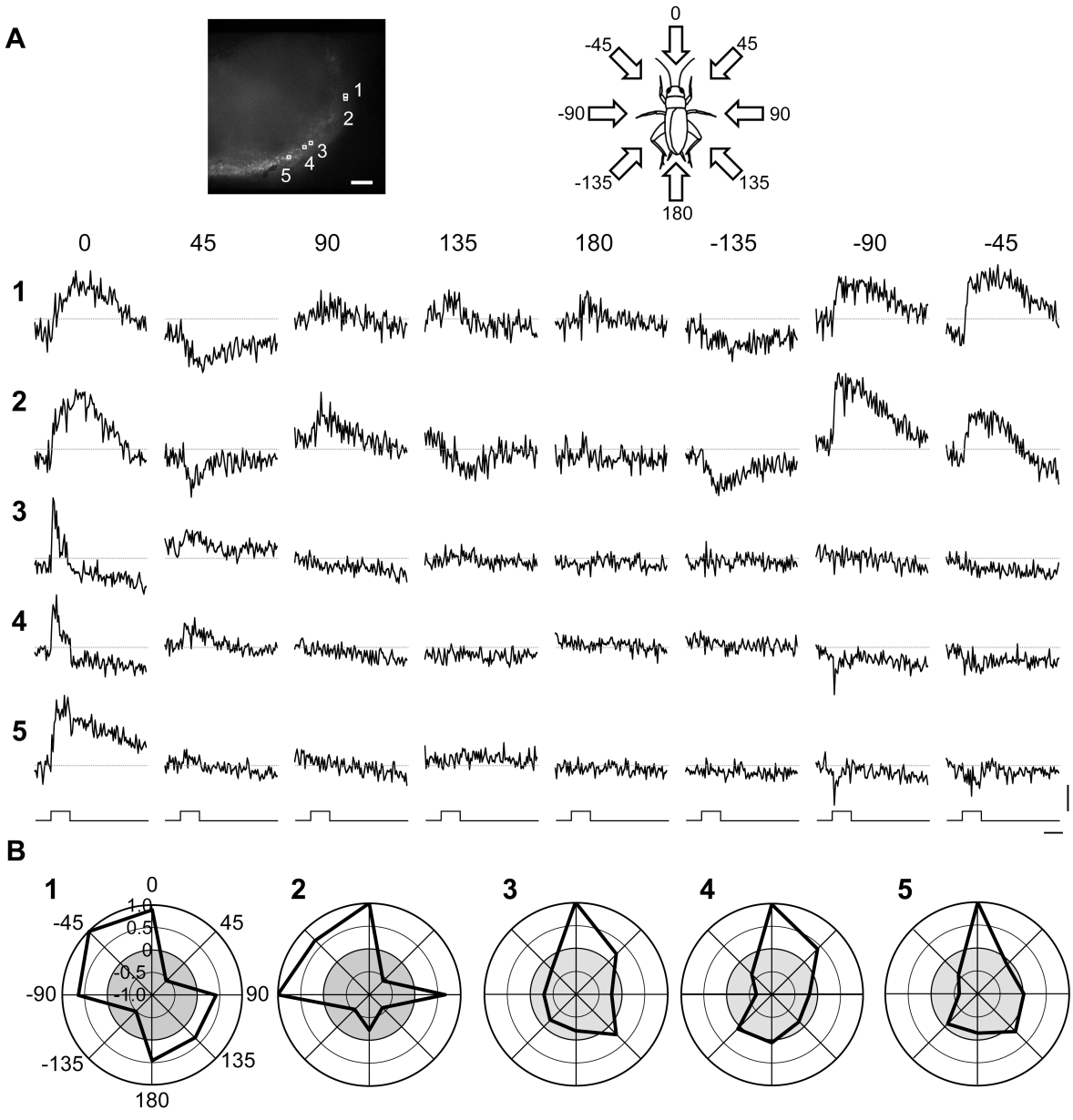
A
1
2
3
4
5
0
-45
45
-90
90
-135
135
180
0
45
90
135
180
-135
-90
-45
B
1
2
3
4
5
1.0
0.5
0
-0.5
-1.0